Opportunistic Doppler-Only Indoor localization via Passive Radar

Li, W., Tan, B. & Piechocki, R.

Original citation & hyperlink:
Li, W, Tan, B & Piechocki, R 2018, Opportunistic Doppler-Only Indoor localization via Passive Radar. in 2018 IEEE 16th Intl Conf on Dependable, Autonomic and Secure Computing, 16th Intl Conf on Pervasive Intelligence and Computing, 4th Intl Conf on Big Data Intelligence and Computing and Cyber Science and Technology Congress(DASC/PiCom/DataCom/CyberSciTech). IEEE, pp. 467-473, The 3rd IEEE Cyber Science and Technology Congress, Athens, Greece, 12/08/18. https://dx.doi.org/10.1109/DASC/PiCom/DataCom/CyberSciTec.2018.00093

DOI 10.1109/DASC/PiCom/DataCom/CyberSciTec.2018.00093
ISBN 978-1-5386-7518-2

Publisher: IEEE

Opportunistic Doppler-Only Indoor localization via Passive Radar

Wenda Li*, Bo Tan†, Robert J. Piechocki*

*Department of Electrical and Electronic Engineering, University of Bristol, UK
†School of Computing, Electronics and Mathematics, Coventry University, UK
*{wenda.li, r.j.piechocki}@bristol.ac.uk,†bo.tan@coventry.ac.uk

***Abstract*—Indoor localization is a vital ingredient for many e-Healthcare and Ambient Assisted Living (AAL) applications. However, accurate, low power and user acceptable solutions remain elusive. In this paper, we present a novel opportunistic system which estimates the localization information based only on the Doppler information from the user. The Doppler information is collected using the passive radar technique that deploys the RF energy transfer signal which originally intended only to deliver energy to home IoT devices. A low complexity Extended Kalman Filter (EKF) is also proposed to predict and track the user's location. A real-time system has been built based on the software defined radio (SDR) platform to verify the proposed methodology. Experimental results indicate that the proposed concepts can be used for indoor localization with a high degree of accuracy.**

***Index Terms*—Doppler Radar, Indoor Localization, Passive Sensing, Extended Kalman Filter**

I. Introduction

The indoor localization provides invaluable information for many application such as Ambient Assisted Living (AAL) systems for the elderly people or location-based services (LBS) for the mobile application and optimization in complex logistics systems, etc. Currently, one of the popular approaches is to use cameras (or depth cameras) which able to provide all levels of accuracy [1]. However, they attract privacy concerns and are limited by lighting conditions. The use of Infrared (IR) for indoor localization by collecting the angular information has been studied in [2], but it is confined by the coverage area which is normally within one single room (with often limited accuracy). Alternatively, the relative distance can be measured by the Time of Arrival (ToA) with the use of Ultra Sound (US) [3]. Yet the temperature and humidity could affect the system performance. In comparison, the passive radar techniques could be used for posture recognition [4] and long-term and large area monitoring with lower privacy concerns and mitigating other issues as mentioned above [5].

Current passive radar systems are mostly used for outdoor target tracking with the television signal [6] or FM radio [7]. This is because of existing commercial signals are relatively narrowband compared to Ultra-Wide-Band (UWB) radar system [8], which results in poor range resolution 6m for GSM and 1.5km for FM. Although the outdoor targets (airplane or ship) can tolerate this deviation, it cannot provide meaningful range information for localization purposes. Previous works [6], [7] show a moving person/subject can be localized by measuring its Doppler information with proper tracking filters. Similar research has been shown in [9] by using the WiFi signal, yet it has limited discussion on the selection of Doppler information. Also, they use high complexity filter which might be problematic in real life applications. Another device-free approach has been shown in [10] by analyzing the perturbation created by a client in the wireless sensor network (WSN). However, it suffers from poor position accuracy at 3-8 meters error and requires more than 15 sensors for a single room. In this work, we present the methodology of a passive radar-based system for indoor localization using an opportunistically signal produced by wireless energy transfer devices [11]. A large area can be covered with only three receivers and able to achieve a high degree of accuracy.

There are two significant challenges need to be solved in our system. The first challenge is how to detect the Doppler information of the target accurately. In this work, we use Cross Ambiguity Function (CAF) [12] to generate the range-Doppler mapping based on the variation of the reflected signal. Then a clean algorithm has been used to remove the direct signal interference and other stationary targets' reflection. After that, a Doppler spectrogram is generated based on a group of CAF mapping. Lastly, we introduce a method to extract the precise Doppler information from Doppler spectrogram. This method could help to reduce the uncertainty in measurement and improve the localization accuracy. The other challenge is the system complexity control. Traditionally, passive radar with tracking filter requires high computing capability and usually a specially designed process unit is needed. In comparison, we use a regular laptop as a processing unit which means the complexity of signal processing needs to be minimized. For passive radar signal processing, batching processing has been used to reduce the computations in correlation and short FFT transformation by cutting received signal into several segmentation [13]. For tracking filters, we introduce a low complexity EKF by converting the transition matrix and observation matrix into sparse matrices instead of matrix multiplication. The proposed method shows 12.3% reduction in computational time.

In comparison to published work [6], [7], [9], the following main contributions are presented:

- We demonstrate the wireless energy transfer signals, aimed at powering energy frugal IoT, can be used op-

portunistically for indoor localization purposes.

- We propose a precise Doppler selection method to improve the Doppler accuracy by examining surround measurements. This method can avoid the Doppler peak due to other parts of the body or irregular source signal.
- To enable real-time processing, we use the batching process to reduce the CAF mapping complexity and introduce a low complexity EKF. The experiment results in section IV-B indicate the proposed methodology has only minor reduction in tracking performance.

The rest of this paper is organized as follow: Section II outlines the signal processing of extracting Doppler information by passive radar; the model structure and mathematical expression for low complexity EKF are presented in Section III; system architecture, experiment result are described in Section IV; conclusions are in Section V.

II. Measurement of Doppler Information

A. Passive Radar Signal Processing

The passive radar system has bistatic geometry: the transmitter and receiver are not co-located. The measurement of Doppler shift allows it possible to estimate its location. The bistatic geometry can be shown as in Fig 1.

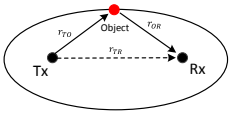

Fig. 1. Bistatic Geometry for Passive Radar

where r_{TO} and r_{OR} is the distance between transmitter to object and object to receiver. For a passive radar system, the path r_{TR} is considered as reference channel, the path r_{OR} is considered as surveillance channel. Note that, the antennas for surveillance and reference channels do not require co-location. But for simplicity, we assume they are in one place. While the object is moving, the Doppler shift f_d (bistatic velocity) of the object can be shown as (1):

$$f_d = \frac{1}{\lambda}\frac{d}{dt}(r_{TO} + r_{OR}) \tag{1}$$

The Doppler shift and the bistatic distance R_b can be obtained with CAF mapping by correlating the surveillance signal and reference signal. In this work, a batching process is applied to CAF mapping to reduce the computational power [12] so that the system can be run in real-time. The CAF mapping with batching process can be expressed as (2):

$$CAF(R_b, f_d) = \sum_{k=0}^{n_b-1} \int_0^{T_i} S_i(t) R_i{}^*(t - kT_B - \frac{R_b}{c}) e^{j2\pi f_c f_d t} dt \tag{2}$$

where S_i and R_i is the obtained signal from surveillance and reference channel after batching process, k is the index of batching, T_i is the integration time, T_B is the batching length (effect the noise level of CAF mapping) and n_b is the number of batching (indicates the maximum detectable speed). The correlation between surveillance and reference signal gives a strong direct signal interference (DSI) that could cover the target and needed to be removed. For this purpose, we implement a CLEAN algorithm introduced in [14] as (3):

$$CAF^k(\hat{R}_b, \hat{f}_d) = CAF^{k-1}(R_b, f_d) - \alpha^k CAF_{self}(R_b - T_k, f_d) \tag{3}$$

where $CAF^k(\hat{R}_b, \hat{f}_d)$ represents the cleaned CAF mapping at k_{th} iteration, α^k is the maximum absolute value of shift factor refers to location of α^k, and CAF_{self} is the self-ambiguity surfaces of the reference channel. Then we pick a column that containing the maximum Doppler peak from one CAF mapping, then combined a group of Doppler peaks to from a spectrogram $D(f_d, n)$ with time index as (4):

$$D(f_d, n) = \sum_{n=0}^{K-1} arg_{f_d}\{max(CAF(R_b, f_d))\} \tag{4}$$

where n is the index of total K recorded CAF mapping, $arg_{f_d}\{max()\}$ gives the column with maximum detected Doppler peak. We plot an example of Doppler spectrogram of a person walking away from the surveillance antenna in Fig 2 from eq (4). As can be seen, there is a clear Doppler trace at 7 Hz that represent human walking speed which becomes visually indistinct after 8 second. This is due to the strength of reflected energy decayed as distance increased. Moreover, although the signal from energy harvesting tends to be more stable than WiFi signal [5], yet it still contains time gap and power fluctuation during transmission. There are two 'bad' time slots which have Doppler shift span across y-axis that resulting in corrupted and unusable Doppler information.

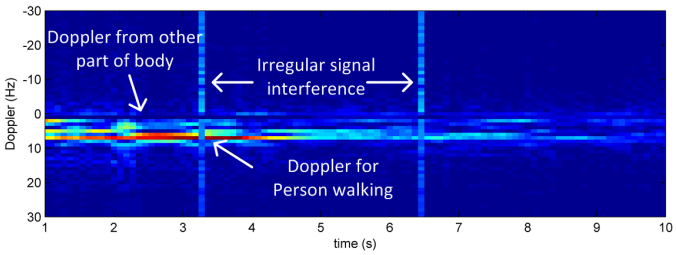

Fig. 2. An example of measured Doppler spectrogram.

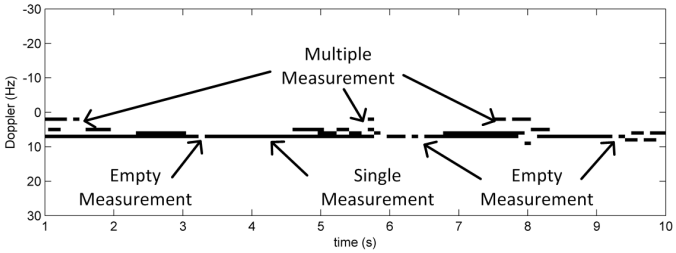

Fig. 3. Corresponding extracted Doppler shift.

B. Precise Doppler Selection Method

The approach described in paper [9] works effectively only if the Doppler information could be extracted accurately. However, from the real measurement, we observe there could

be multiple interferences that affect this process. As the Doppler peak does represent not only the target's velocity but also the frequency from other parts of the bodies such as head, arm and leg. But in this work, we only consider the velocity of the target. Therefore those unrelated Doppler peaks should be removed. Furthermore, we also need to consider the interference from the irregular source signals.

Here we present a procedure to eliminate these interference and extract the precise Doppler information. Starting with traditional radar method by using the constant false alarm rate (CFAR) to detect the target by generating a threshold mapping $T(i,j)$ based on the cleaned CAF mapping $CAF(i,j)$ with l range bin and m Doppler bin as (5):

$$T(i,j) = \sum_{l=1}^{N_L} \sum_{m=1}^{N_M} (|CAF(i \pm l, j \pm m)|)^2 \tag{5}$$

Then a target could be determined by: $CAF(i,j) - T(i,j) > 0$. The corresponding extracted Doppler peak is shown at Fig 3. As can be seen, the traditional method can only provide a rough image about the velocity: there are three different type of Doppler measurements that need to be selected separately. The first type measurement is when single velocity is captured at a certain time, this is the simplest case as the Doppler peak is unique, therefore we can confidently extract the velocity $v_{(k,1)}$ as (6):

$$v_{(k,1)} = [D]_{n=k}^{f_d} \tag{6}$$

where ($[D]_{n=k}^{f_d}$ donates the detected Doppler peak at time k). The second type measurement happens when no Doppler peak is detected. There are two possible reasons: (1) the target is in stationary or (2) CAF fails in detecting the target due to 'bad' time slot or low reflect power. For this type measurement, we exam the empty slot by searching forward and backward velocity to decide most possible situation for velocity $v_{(k,2)}$:

$$v_{(k,2)} = \frac{1}{2}\left([D]_{n=k-1}^{f_d} + [D]_{n=k+1}^{f_d}\right) \tag{7}$$

If consecutive measurements are zeros, we assume the target is in stationary. Otherwise, we calculate the mean value to replace the empty measurement. The third type measurement includes multiple Doppler peaks in a one time-slot. It is more complicated and much difficult to decide the object's velocity. As there are many possible elements cause the multiple measurements, for example, the CFAR also captures Doppler shift from other parts of a body, or the DSI process does not clean the CAF mapping completely. In addition, we observe this type of measurement usually span over several time-slots (Fig 3) which further increase the uncertainty. Traditional CFAR picks the Doppler peak with the largest value, but it does not solve the problem as the sidelobe usually contains more power than a target. In this work, we calculate the weighed of each peak to search the most likely velocity. The first step is to calculate a weight vector W which consists the amplitude value of each row in the $D(f_d, n)$ over a period of time T_W as T_W as $W(f) = \sum_{n=0}^{T_W} D(f,n)$. For consistency, T_W is chosen as the same length as integration time T_i. Then we decide the velocity $v_{k,3}$ by calculating the difference of each Doppler peak compare with weight vector as (8):

$$v_{(k,3)} = min(\sum_{f=-n_b/2}^{n_b/2} (W(f) - [D]_{n=k}^{f_d})^2) \tag{8}$$

where $min(.)$ means to select the Doppler peak with the smallest difference to weight vector. Note that the number of batch n_b also defines the size of Doppler boundary. The effectiveness of proposed Doppler information extraction will be shown in Section IV-A.

III. Localization with DopplerOnly

A. Model Description

Let us define the object moving in a finite 2D space with following parameters: x_k and y_k are the Cartesian coordinates for the target position at time of k, $v_{x,k}$ and $v_{y,k}$ are the target velocity at x-axis and y-axis. The target can then be expressed as (9):

$$\boldsymbol{x}_k = [x_k, y_k, v_{x,k}, v_{y,k}]^T \tag{9}$$

where T is the transpose operation and $\boldsymbol{x}_k$ is the state vector. The state transition function can be expressed as (10):

$$\boldsymbol{x}(k) = F_{k|k-1}\boldsymbol{x}(k-1) + w(k) \tag{10}$$

where $F_{k|k-1}$ is the state transition model:

$$F_{k|k-1} = \begin{bmatrix} I_{(2\cdot 2)} & I_{(2\cdot 2)}\Delta T \\ 0_{(2\cdot 2)} & I_{(2\cdot 2)} \end{bmatrix} \tag{11}$$

where ΔT is the step time or system measurement rate. $w(k)$ represents the processing noise for $\boldsymbol{x}_k$, according to [15], it is modeled as uncorrelated Gaussian model $w(k) \sim N(v, Q)$, Q is the covariance matrix given as (12):

$$Q = \sigma_v^2 \begin{bmatrix} I_{(2\cdot 2)}Q_1 & I_{(2\cdot 2)}Q_2 \\ I_{(2\cdot 2)}Q_3 & I_{(2\cdot 2)}Q_4 \end{bmatrix} \tag{12}$$

where σ_v^2 is the standard deviation of the model noise, and $Q_1 = \Delta T^4/4$, $Q_2 = Q_3 = \Delta T^2/2$ and $Q_4 = \Delta T^3/2$. The noisy observation model with m-th receiver can be then expressed with following equation (13):

$$Z_m(k+1) = h_m(\boldsymbol{x}(k)) + \varepsilon_k \tag{13}$$

where ε_k is the uncorrelated measurement noise and function $h_m(\boldsymbol{x}(k))$ is the Doppler measurement as (14);

$$h_m(\boldsymbol{x}(k)) = \left\{\frac{v_{x,k}(x_k - x_T) + v_{y,k}(y_k - y_T)}{\lambda r_{TO}}\right\} + \left\{\frac{v_{x,k}(x_k - x_m) + v_{y,k}(y_k - y_m)}{\lambda r_{OR}}\right\} \tag{14}$$

where x_T, y_T is the position of energy harvesting transmitter and x_m, y_m is the position of mth receiver. λ is wavelength of the signal.

B. Tracking with Low Complexity EKF

According to equation (14) the measurements are nonlinear, therefore we cannot direct use the Kalman filter. Alternatively, EKF process the first order of the nonlinear measurement into linear version. Due to the bandwidth of available signal, the

measurement on x_k and y_k are too coarse for indoor scenario. However, previous work shows the passive radar could achieve high Doppler resolution [13], [15]. After removal the bistatic range components, the measurement model is given as: $h_m(x_k) = v_m(x_k)$. The Taylor expansion introduced by [16] has been used, and the Jacobian matrix of $h_m(x_k)$ can be expressed as (15):

$$J_h^m(x) = \left[\frac{\delta h_m(x_k)}{\delta x_k}\frac{\delta h_m(x_k)}{\delta y_k}\frac{\delta h_m(x_k)}{\delta v_{x,k}}\frac{\delta h_m(x_k)}{\delta v_{y,k}}\right] \quad (15)$$

In the Doppler only EKF, an assumption has been made: the start point of the target is known. In real application, this could be achieved by other method, for example, the start point could be assume at the entry of the room. The initial state vector can be denoted as: $\boldsymbol{x}_0 = [x_0, y_0, v_{x,0}, v_{y,0}]^T$, the prediction steps of standard EKF are:

$$\hat{x}_k = F_{k|k-1}\hat{x}_{k-1} \quad (16)$$
$$\hat{P}_k = F_{k|k-1}\hat{P}_{k-1}{F_{k|k-1}}^T + Q \quad (17)$$
$$K_k = P_k H_k^T (H_K \hat{P}_k H_K^T + \xi_k)^{-1} \quad (18)$$

Then the update steps are:

$$x_k = \hat{x}_k + K_k(z_k - h(\hat{x}_k)) \quad (19)$$
$$P_k = (I - K_k H_k)\hat{P}_k \quad (20)$$

We propose the low complexity EKF based on the sparse matrix calculation [17]. As we know the matrix F is a sparse matrix with 1 in diagonal elements. Thus the multiplication of ${F_{k|k-1}P_{k-1}F_{k|k-1}}^T$ in eq (17) can be simplified into:

$$\hat{P}_k = \begin{bmatrix} Q_1 + (Q_1 + Q_3)\Delta T + Q_3\Delta T^2 & Q_2 + Q_4\Delta T \\ Q_3 + Q_3\Delta T & Q_4 \end{bmatrix} + Q \quad (21)$$

The product in eq (21) is a sparse matrix, so that the complexity of eq (18) is reduced due to both $\hat{P}_k$ and H_k are sparse matrix. The matrix calculation on $H_K\hat{P}_k H_K^T$ gives a diagonal matrix R with size of $(2 \cdot 2)$, and it is much computational efficient in the inverse matrix calculation. The eq (18) can be then simplified as:

$$K_k = P_k \begin{bmatrix} 0_{(2\cdot 2)} \\ (R + \xi_k)^{-1} \end{bmatrix} \quad (22)$$

and the eq (20) can be simplified to:

$$P_k = (I - [0_{(4\cdot 2)} \quad K])\hat{P}_k \quad (23)$$

We compare the complexity of standard EKF and the proposed low complexity EKF base on the number of multiplication and addition as shown in Table I, where n is the number of states and m is the number of variables (in our application, n=4 and m=2). As can be seen, the low complexity EKF significant reduces the amount in both multiplication and addition. The total number of low complexity EKF is 104 in multiplications and 28 in additions that give 68% and 79% reduction compare to standard EKF. Then we test the computational performance of both filters with MATLAB. The result shows 5.45 ms is required by standard EKF for one iteration, whereas the proposed low complexity EKF is 4.78 ms that gives 12.3% in time reduction. The performance is expected to be more significant when the system has more state and variable.

TABLE I
COMPARISON OF MATRIX COMPUTATION BETWEEN STANDARD EKF AND LOW COMPLEXITY EKF

Standard EKF	(17)	(18)	(20)	total
Multiplication Number	$2n^3$	$2n^2m + 2m^2n$	$n^3 + n^2m$	320
Addition Number	$2n^2$	$2n^2m + 2m^2$	$2n^2$	136
Low Complexity EKF	(21)	(22)	(23)	
Multiplication Number	$2n$	n^2m	n^3	104
Addition Number	n	nm	n^2	28

IV. EXPERIMENTS & RESULTS

We have built a passive system based on our previous work [12] with three USRP-2920 [18] for collecting the signal. A signal distribution system [19] has been used to share the clock for USRP for synchronization purpose. The received signal is then transferred to a laptop (process unit) via Ethernet port. The signal processing described in previous sections are implemented with LabVIEW™. To further reduce the real-time latency, the signal processing is designed with pipeline structure [13] so that we could divide a large task into multiple sub-procedures. Also, a graphics control center is built to allow the user to control the system and display result.

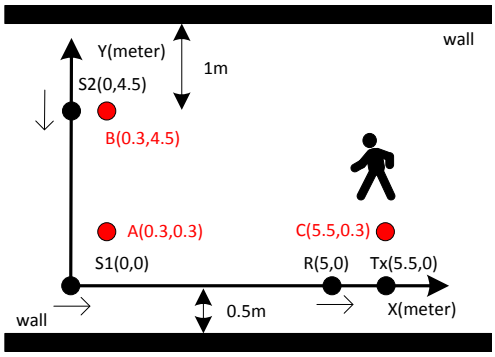

Fig. 4. Experiment layout.

The experiment is carried out in a lab room. The layout is shown in Fig 4. Point R, S1, S2 are the reference and monitoring antenna with position (5,0), (0,0), (0,4.5), the energy harvesting transmitter Tx is located at (5.5,0). Two monitoring antenna S1 and S2 are pointed to X and Y perpendicular to the monitoring area, whereas the reference antenna R is led to the transmitter. We set three test point as A(0.3,0.3), B(0.3,4.5), C(5.5,0.3), a person is asked to moving between those points, the test path will be explained in the different experiment.

A. Experiment 1: Effectiveness of Proposed Precise Doppler Selection

In this experiment, we present the localization performance with & without the proposed Doppler selection. Two tests have been carried out to validate the location accuracy with standard EKF. In the first test, a person was asked to walk through the path: $C \rightarrow A \rightarrow B$ with same relative speed

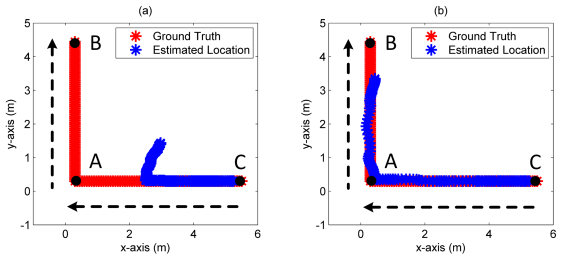

Fig. 5. Tracking result at 0.1s step time of straight path (a) with CFAR only, (b) with precise Doppler selection.

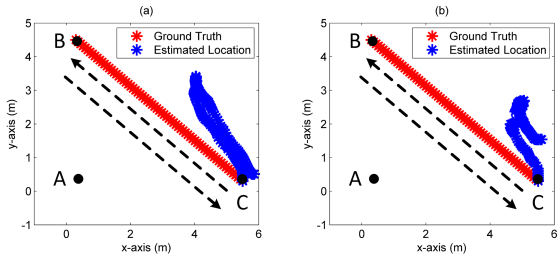

Fig. 6. Tracking result at 0.1s step time of diagonal path (a) with CFAR only, (b) with precise Doppler selection.

TABLE II
MSE RESULTS WITH & WITHOUT DOPPLER SELECTION METHOD OF STRAIGHT PATH

Step Time (T)	Without Doppler Selection	With Doppler Selection
0.01	1.1614	0.4588
0.1	1.2992	0.6134
0.3	1.5350	1.1984
0.5	1.9737	1.3958
1	2.5944	2.4056

TABLE III
MSE RESULTS WITH & WITHOUT DOPPLER SELECTION METHOD OF DIAGONAL PATH

Step Time (T)	Without Doppler Selection	With Doppler Selection
0.01	1.8508	1.1337
0.1	2.2741	1.5696
0.3	2.3968	1.8182
0.5	2.4784	1.9185
1	2.7760	2.0145

(labeled as the black arrows). The CAF mapping is processed with 1s of integration time and 0.1s of step time offline. The tracking results are shown in Fig 5: (a) with CFAR only, (b) with precise Doppler selection. As can be seen, the proposed method largely improves the localization performance. The tracking path in Fig 5(a) shows some Doppler information detected by CFAR are not present the user's velocity which causes errors in location estimation. In both x-axis and y-axis, estimated path are shorter than the ground truth. The tracking path in Fig 5(b) shows much better estimation than Fig 5(a) which proves the precise Doppler selection method is needed. However, more noise is observed in x-axis than y-axis. This is because the direction changed suddenly, it takes more process to update the path for EKF, while in the y-axis, the velocity is more constant from the beginning. Another critical factor is the geometry of the system, as the surveillance antenna S1 points to the Tx that receives more power than S2 which explain the performance variation in x-axis and y-axis.

The mean-square-error (MSE) is calculated between ground truth and estimated location to present the accuracy. The MSE result versus step time is shown in Table II. As can be seen, the MSE increased together with step time as expected. Also, there is substantial MSE error difference between with & without Doppler selection especially in small step time and less variation in considerable step time. This is because of the significant step time itself introduce significant MSE, whereas the proposed Doppler selection has less effect on the tracking when the step time is not sufficient.

The walking path in the first test is comparably simple with 0 or 90 degrees angular towards both surveillance antenna which means the relative velocity is more persistent. In this test, we test the tracking performance under a diagonal path as $C \rightarrow B \rightarrow C$. For both antenna, the angle of walking path changes continuously, which increases the tracking complexity as the measured velocity is varied through the Doppler spectrogram yet the actual speed remains same. The tracking results are shown in Fig 6. As can be seen, both paths contain variation in direction and also shorter compare with the ground truth. This is because the antenna receive less signal power when the angle is small, and CFAR cannot detect the target. However, with the Doppler selection, the tracking path shows the user back to the start point as expected, whereas the tracking path without Doppler selection shows more randomness and a significant separation between the start point and end point.

The MSE for diagonal walking is shown in Table III. As can be seen, the MSE for the diagonal path is much higher than that in the straight path. Even at 0.01s step time, the MSE remains at high level. The main reason for this downgrade in performance is because of the insufficient Doppler measurement which can hardly correct from filter side. One of the possible solutions is to increase the number of surveillance channel so that we could improve the accuracy in detection of Doppler.

B. Experiment 2: Localization over Long Period

Since our system is capable of real-time Localization. In this experiment, we would like to exam the proposed system over a long period. The performance of standard EKF and low complexity EKF will also be tested. Currently, our system has the real-time limitation at 0.3s step time with integration time at 1s. A person was asked to walk continuously with path $C \rightarrow A \rightarrow B \rightarrow A \rightarrow C$ and another person recorded the time duration of the walking path to generate ground truth. The period of the measurement is 3 minutes. We plot the tracking path in Fig 7 (a) standard EKF, (b) low complexity EKF. As can be seen, both filter shows almost same tracking path which indicates the proposed low complexity EKF has similar performance to the standard EKF. Moreover, both tracking path shows some reduction in x and y-axis estimation

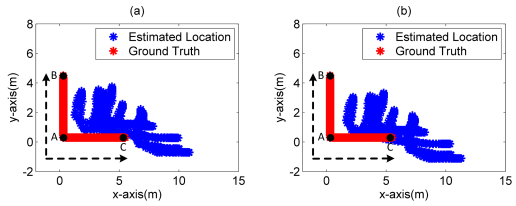

Fig. 7. Tracking Result over 3 minutes with (a) standard EKF, (b) low complexity EKF.

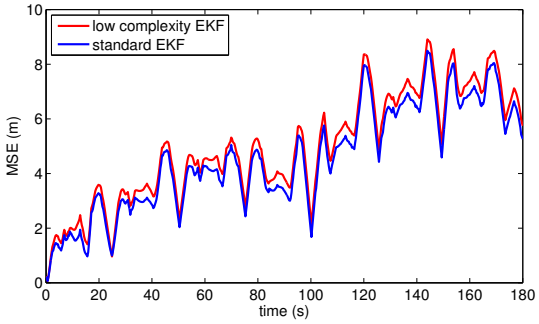

Fig. 8. MSE versus time.

compares to Fig 5. It is because of the longer step time increases its MSE according to Table II and III. Furthermore, the offset of cyclical walking indicates there is an accumulated error during the tracking process.

To better compare the tracking performance of both filter, we plot the MSE versus time and plot in Fig 8. As can be seen, the MSE for both filter increased over time in general. The standard EKF shows slightly better MSE than the proposed low complexity EKF. The reason is due to the matrix simplification on eq (21) and eq (23) that could filter out some information. Furthermore, a 'reset' action is essential for our system. Due to the MSE accumulates over the time, the 'reset' action could clear the MSE so that the tracking performance can maintain at high accuracy.

V. Conclusions

In this work, a real-time indoor localization system has been presented. It shows a different approach compare to previous work [1], [8], [10] with advantages as opportunistic, wide deployable and low privacy issue. For the system, two major challenges are Doppler information extraction and system complexity. We describe a novel procedure of using passive radar principle to detect object's velocity. Then we proposed a precise Doppler selection method to improve the accuracy, the effectiveness of this process is shown in Section IV-A. Also, the experiment results indicate the tracking system has good performance in zero angular path towards surveillance antenna, however, when the angle is changed the tracking error is increased. In addition, a low complexity EKF has been proposed by converting state and observer matrix into sparse matrices and shows 12.3% time reduction, yet provides almost same tracking performance compared to standard EKF. Moreover, the experiment results in Section IV-B illustrate accumulative error in our system. Future work will include the research of possible 'reset' action by using information fusion with other sensors which can improve the tracking performance and make the system more robust. In the future work, we need to investigate the performance of the system in empty room and room with fornitures to verify the robustness of the system in multiple environment.

Acknowledgments

This work was partially funded under the SPHERE IRC, the UK Engineering and Physical Sciences Research Council (EPSRC), Grant EP/K031910/1.

References

[1] R. Mautz and S. Tilch, "Survey of optical indoor positioning systems," in *Indoor Positioning and Indoor Navigation (IPIN), 2011 International Conference on*, Sept 2011, pp. 1–7.

[2] K. Atsuumi, M. Hashimoto, and M. Sano, "Optical azimuth sensor for indoor mobile robot navigation," in *Computer Engineering Systems, 2008. ICCES 2008. International Conference on*, Nov 2008, pp. 381–386.

[3] M. Alloulah and M. Hazas, "An efficient cdma core for indoor acoustic position sensing," in *Indoor Positioning and Indoor Navigation (IPIN), 2010 International Conference on*, Sept 2010, pp. 1–5.

[4] S. A. Shah, N. Zhao, A. Ren, Z. Zhang, X. Yang, J. Yang, and W. Zhao, "Posture recognition to prevent bedsores for multiple patients using leaking coaxial cable," *IEEE Access*, vol. 4, pp. 8065–8072, 2016.

[5] W. Li, B. Tan, R. J. Piechocki, and I. Craddock, "Opportunistic physical activity monitoring via passive wifi radar," in *e-Health Networking, Applications and Services (Healthcom), 2016 IEEE 18th International Conference on*, Sep 2016.

[6] A. Amar and A. J. Weiss, "Localization of narrowband radio emitters based on doppler frequency shifts," *IEEE Transactions on Signal Processing*, vol. 56, no. 11, pp. 5500–5508, Nov 2008.

[7] P. E. Howland, "Target tracking using television-based bistatic radar," *IEE Proceedings - Radar, Sonar and Navigation*, vol. 146, no. 3, pp. 166–174, Jun 1999.

[8] S. Kumar, S. Gil, D. Katabi, and D. Rus, "Accurate indoor localization with zero start-up cost," in *Proceedings of the 20th Annual International Conference on Mobile Computing and Networking*, ser. MobiCom '14. New York, NY, USA: ACM, 2014, pp. 483–494. [Online]. Available: http://doi.acm.org/10.1145/2639108.2639142

[9] Q. Chen, B. Tan, K. Woodbridge, and K. Chetty, "Indoor target tracking using high doppler resolution passive wi-fi radar," in *2015 IEEE International Conference on Acoustics, Speech and Signal Processing (ICASSP)*, April 2015, pp. 5565–5569.

[10] S. Tennina, R. Alesii, F. Tarquini, and F. Graziosi, "Indoor localization solutions to support independent daily life of impaired people at home," in *2016 IEEE International Conference on Communications Workshops (ICC)*, May 2016, pp. 45–50.

[11] Powercast energy harvesing transmitter. [Online]. Available: http://www.powercastco.com/products/powercaster-transmitter

[12] W. Li, B. Tan, and R. J. Piechocki, "Non-contact breathing detection using passive radar," in *2016 IEEE International Conference on Communications (ICC)*, May 2016, pp. 1–6.

[13] B. Tan, K. Woodbridge, and K. Chetty, "A real-time high resolution passive wifi doppler-radar and its applications," in *2014 International Radar Conference*, Oct 2014, pp. 1–6.

[14] K. Kulpa, "The clean type algorithms for radar signal processing," in *Microwaves, Radar and Remote Sensing Symposium, 2008. MRRS 2008*, Sept 2008, pp. 152–157.

[15] M. Wielgo, P. Krysik, K. Klincewicz, L. Maslikowski, S. Rzewuski, and K. Kulpa, "Doppler only localization in gsm-based passive radar," in *2014 International Radar Conference*, Oct 2014, pp. 1–6.

[16] G. Welch and G. Bishop, "An introduction to the kalman filter," Chapel Hill, NC, USA, Tech. Rep., 1995.

[17] J. Z. Sasiadek, A. Monjazeb, and D. Necsulescu, "Navigation of an autonomous mobile robot using ekf-slam and fastslam," in *Control and Automation, 2008 16th Mediterranean Conference on*, June 2008, pp. 517–522.

[18] Ni usrp 2921. [Online]. Available: http://sine.ni.com/nips/cds/view/p/lang/en/nid/212995

[19] Octoclock cda-2990. [Online]. Available: https://www.ettus.com/product/details/OctoClock